Materials Physics and Mechanics. 2022;50(2): 287-303
Research article
http://dx.doi.org/10.18149/MPM.5022022_9

Submitted: July 19, 2022
Approved: August 22, 2022
Accepted: August 25, 2022

Hybrid modeling of gas-dynamic processes in AC plasma torches

N.Y. Bykov[1,2], N.V. Obraztsov[1,2]✉, A.A. Hvatov[2], M.A. Maslyaev[2], A.V. Surov[2,3]

[1]Peter the Great St. Petersburg Polytechnic University, 29 Politechnicheskaya st., St. Petersburg, 195251, Russia

[2]ITMO University, 49 Kronversky av., St. Petersburg, 197101, Russia

[3]Institute for Electrophysics and Electric Power RAS, 18 Dvortsovaya emb., St. Petersburg, 191186, Russia

✉ nikita.obrazcov@mail.ru

Abstract. A model of plasma-forming gas flows in AC plasma torches was proposed for the range of operating parameters typical for technologies for the synthesis of perspective materials. It assumes the solution of the Navier-Stokes equations together with the equation for the electric field potential and includes a model of arc root motion. The law of the motion was restored by the method of generative model design from the available experimental data. The COMSOL Multiphysics^R package was used for simulations. An additional analysis of the applicability of various package modules for modeling essentially subsonic compressible flows with energy release was carried out. Recommendations were given for the simulation of flows in AC plasma torches. The influence of the arc root motion on the flow pattern was studied and the significant asymmetry in the gas-dynamic parameter distributions was shown.
Keywords: AC plasma torch, model of plasma-forming gas flow, arc root motion, method of generative model design, energy release into flow

Acknowledgements. *This research is financially supported by The Russian Science Foundation, Agreement No. 21-11-00296, https://rscf.ru/en/project/21-11-00296/*
The computation resources were provided by the Supercomputer Center of Peter the Great St. Petersburg Polytechnical University.
The authors express their gratitude to the engineers of the Russian office of COMSOL Multiphysics^R, Dmitry Lazarev and Sergey Yankin for valuable comments on the problem statement.

Citation: Bykov NY, Obraztsov NV, Hvatov AA, Maslyaev MA, Surov SA. Hybrid modeling of gas-dynamic processes in AC plasma torches. *Materials Physics and Mechanics*. 2022;50(2): 287-303. DOI: 10.18149/MPM.5022022_9.

1. Introduction

The development of technologies for the synthesis and processing of new materials is associated with the engineering of complex technical devices. Such devices include plasma torches [1-3]. Plasma torches are used for the synthesis of different carbon structures and metal nanoparticles, obtaining dispersed materials including refractory and hard-metal powders, waste processing, as well as for melting, cutting, and heat treatment [3-13]. Alternative current (AC) plasma torches hold a special place in plasma technologies. The possibility of use in industrial premises with no specially developed complex power sources, the ability to work on multispecies plasma-forming media, and the high service life of electrodes are the main advantages of the AC plasma torches [14].

The efficiency of plasma technologies depends on the parameters of the plasma flow that affect the yield of the synthesized material, the quality of welds, the porosity and adhesion of sprayed coatings, the percentage of waste destruction, etc. Optimization of existing and development of new plasma technologies require a tool for estimating the gas-dynamic parameters of the plasma flow (temperature, velocity, density) in the "working" volume. Depending on the type of technology, the "working" volume can serve the internal channels of the plasma torch, the region of jet expansion in the reactor external with respect to the channels, or both regions simultaneously [15]. An experimental study of high-enthalpy flows is difficult due to high gas temperatures in the arc and reactor. Simulation of plasmodynamic processes is associated with a number of computational problems. It is necessary to consider a hybrid problem involving at least three related subproblems: gas-dynamic, thermal, and electromagnetic.

COMSOL Multiphysics, ANSYS Fluent, Code_Saturne, and OpenFOAM are the most frequently used software products for plasmodynamic process simulation [16-21]. The development of existing scenarios for calculating processes in AC plasma torches using these packages requires an understanding of physical aspects, the correct choice of calculation modules, and subsequent fine matching of computational parameters.

An important feature of modeling flows with energy release, namely, Joule heating, is the need for correct consideration of the effects of medium compressibility. In the COMSOL Multiphysics environment, it is possible to use the Laminar/Turbulent Flow modules with the Compressible Flow option, or the High Mach Number Flow module [22] to take into account the compressibility of the flow. In the context of solving the problem with the COMSOL Multiphysics package, a comparative analysis of the results of applying these modules is required. Carrying out such an analysis is one of the goals of this work.

An important element of the hybrid model describing plasmodynamic processes is the arc root motion model. The movement of the arc root depends on many parameters, among the swirling of the gas flow at the channel inlet and the action of an external magnetic field can be distinguished. In the case of a direct current (DC) plasma torch, accounting for the motion of the arc root results in the asymmetry of the instantaneous distributions of parameters in the cross sections of the plasma flow in the channel. In this case, the averaging of spatially asymmetric profiles over time leads to the Gaussian form of the distribution of parameters along the radial coordinate [23]. For an AC plasma torch, the influence of the arc attachment motion on the flow pattern, both in the channel and in the region of jet expansion in the reactor zone, is more complex and insufficiently studied.

To calculate the motion of the arc attachment in the general case, it is additionally necessary to consider the electrical problem for the electrode itself [23], the processes in the near-electrode plasma layer [24], etc. Thus, the solution of the complete problem requires additional computational resources. One of the alternative approaches is the method proposed in this paper for including the law of motion of the arc root into the hybrid model. The law of motion can be reconstructed from the available experimental data using generative model design (GMD) methods in the form of a differential equation (DE) [25-27]. This approach has been implemented and discussed in this paper.

The aim of the work is to develop a model of an AC plasma torch for the simulation of gas-dynamic and electrical parameters in the volume of channels and in the region of gas expansion using the COMSOL Multiphysics package. The proposed study consists of several parts: an analysis of the parameters of a compressible flow in the presence of an energy release, a consideration of the general formulation of the problem, a description of the application of the GMD method to the problem of restoring the law of motion of an arc root in the form of a DE, a discussion of the results of modeling the compressible flow of a plasma-forming gas using various approaches in the COMSOL Multiphysics environment, analysis of

the results of the 3D simulation with regard to the motion of the arc root along the surface of the electrode.

2. Compressibility of the medium in the simulation of AC plasma torches

To estimate the change in pressure, density, and velocity of a medium during its heating in a given temperature range, it is worth having approximate theoretical expressions presented in this section.

It is known that for an isentropic flow, a variation in the Mach number in the range from 0 to 0.14 results in a change in the gas density by 1%. The gas can approximately be considered an incompressible medium with $\rho = const$. In the case of the gas flow in the plasma torch channel, the medium is heated due to the release of Joule heat, and the flow as a whole is significantly non-isentropic. A simplified one-dimensional model of gas flow in a channel, which assumes energy release into the flow in a certain very small spatial region, is considered in [28]. Before and after the energy deposition region, the flow is assumed to be isentropic. Assuming that in area 1 before the heating zone and in area 2 after it, the flow remains substantially subsonic, i.e. corresponding Mach numbers $M_1 << 1, M_2 << 1$, using the theory [28], we have simple relations

$$\frac{M_2}{M_1} \approx \sqrt{\frac{T_2}{T_1}}, \ \frac{p_2}{p_1} \approx 1, \ \frac{\rho_2}{\rho_1} \approx \frac{T_1}{T_2}, \tag{1}$$

where T_i, p_i, ρ_i are the temperature, pressure, and density in area *i* of the channel.

Air heating in AC plasma torches is accompanied by an increase in temperature above 3500-4000K, which is necessary for sufficient conductivity of the medium. Assuming air heating from $T_1 = 300\ K$ to $T_2 = 6000\ K$ in the arc, i.e.

$$\frac{T_2}{T_1} = 20, \ \sqrt{\frac{T_2}{T_1}} = 4.47$$

we get

$$\frac{\rho_2}{\rho_1} \approx \frac{T_1}{T_2} = 0.05.$$

With such a significant change in density, the compressibility of the gas cannot be neglected. With the indicated increase in temperature for a one-dimensional flow, a proportional increase in velocity and a decrease in density occurs

$$\frac{u_2}{u_1} = \frac{\rho_1}{\rho_2} \approx \frac{T_2}{T_1} = 20.$$

The compressibility of a medium in the COMSOL Multiphysics 6.0 environment can be taken into account by the modules (a) Single phase flow, compressible flow, non-isothermal flow (hereinafter referred to as the LF approach), or (b) High Mach number flow (hereinafter referred to as the HM approach). The LF approach is used to calculate a compressible medium at Mach numbers less than 0.3 (which corresponds to the flow conditions in a plasma torch). It is assumed that the medium is "dynamically" weakly compressible, i.e. the change in density due to a change in pressure in the flow does not exceed 5%. In this case, the density may change due to temperature dependence. The implemented numerical schemes for the LF approach do not enable us to determine accurately the propagation of pressure waves [29]. The HM approach can be used to calculate a compressible medium at any Mach number. Spasmodic and sharp parameter changes are permissible. The HM module implements a special solution stabilization algorithm [29].

Analysis of the features of the application of these approaches to solving the problem of modeling the flow in an AC plasma torch is one of the goals of this work.

3. Statement of the problem

The geometry of the problem. The paper considers two geometries of the plasma torch (Fig. 1). In scheme 1, the plasma torch channel contains a cylindrical body, and the end surface AB is the first electrode. In scheme 2, the first electrode is hollow and its surface AB coincides with the inner surface of the channel. The second grounded electrode is in the jet expansion region.

Channel radius is $R_c = 16\ mm$, channel length is 330 mm, and distance from the outlet section of the channel to the electrode in the channel is 240 mm. In the case of a hollow electrode (scheme 2), this is the distance from the outlet section to point B of the hollow electrode. The distance between the electrodes is $L_e = 560\ mm$. For scheme 1 inner cylinder radius is $R_e = 10\ mm$. Jet expansion region has dimensions $L_R = 60R_c$ and $H = 50R_c$ for scheme 1, and $L_R = 20R_c$ and $H = 12.5R_c$ for scheme 2.

Scheme 1 assumes an axisymmetric formulation of the problem, scheme 2 assumes a 3D formulation of the problem by taking into account arc root motion (see subsection below).

Table 1 shows the data on the simulation cases, including the average gas velocity at the channel inlet, the flow rate of the plasma-forming gas (air), and the Reynolds number values.

Table 1. Simulation cases

Case	Electrode	Arc root	Scenario	Scheme	I_0, A	V_{x_in}, m/s	T_{in}, K	Re	G, g/s
A	Cylinder face	Fixed	LF	1	10	1	300	~450	0.568
B	Cylinder face	Fixed	HM	1	10	1.075	300	~480	0.578
C	Hollow	Moving	HM	2	10	1.075	300	~1290	0.975

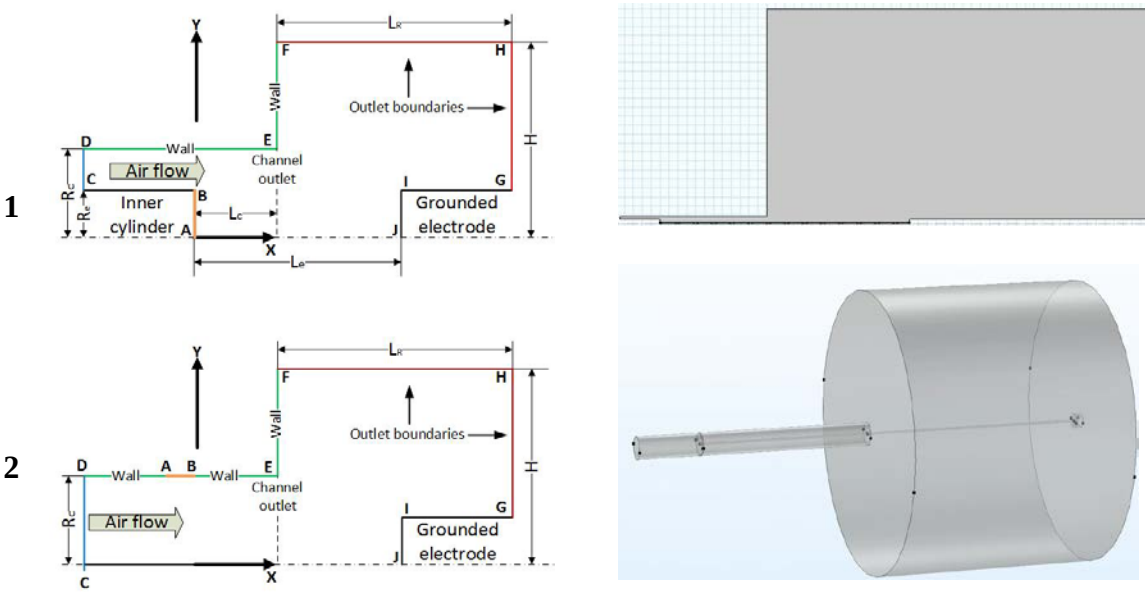

Fig. 1. The geometry of the problem

Mathematical model. The laminar flow of a compressible viscous heat-conducting medium (air) in an alternating electric field is considered. The dynamics of the medium is described by the system of Navier-Stokes equations [22]:

$$\frac{\partial \rho}{\partial t} + \nabla \cdot (\rho \mathbf{u}) = 0, \tag{2}$$

$$\rho\left(\frac{\partial \mathbf{u}}{\partial t} + (\mathbf{u} \cdot \nabla)\mathbf{u}\right) = \nabla \cdot (-p\mathbf{I} + \tau), \tag{3}$$

$$\tau = \mu(\nabla\mathbf{u} + (\nabla\mathbf{u})^T) - \frac{2}{3}\mu(\nabla\cdot\mathbf{u})\mathbf{I},$$
$$\rho C_p\left(\frac{\partial T}{\partial t} + (\mathbf{u}\cdot\nabla)T\right) = -(\nabla\cdot\mathbf{q}) + \tau:\mathbf{S} - \frac{T}{\rho}\frac{\partial\rho}{\partial T}\Big|_p\left(\frac{\partial p}{\partial t} + (\mathbf{u}\cdot\nabla)p\right) + Q_J, \quad (4)$$
$$\mathbf{q} = -\lambda\nabla T,$$

where t is the time; $\mathbf{u}$ is the velocity; ρ, p, and T are the density, pressure, and temperature of the medium, respectively; τ is the viscous stress tensor; $\mathbf{q}$ is the heat flow vector; $\mathbf{S}$ is the strain-rate tensor: $\mathbf{S} = (\nabla\mathbf{u} + (\nabla\mathbf{u})^T)$; $Q_j = \mathbf{j}\cdot\mathbf{E}$ is the Joule heating power ($\mathbf{j}$ is the current density, $\mathbf{E}$ is the electric field strength); C_p is the heat capacity at constant pressure, μ is viscosity and λ is heat conduction coefficient.

Equation (4) accounts for the work of viscous friction forces and pressure forces. Radiation of heated air in the considered temperature range is disregarded. Air is considered in the single-fluid approximation. The molar mass of air M_a and its other thermophysical parameters (thermal conductivity, heat capacity) are functions of temperature. Density, pressure, and temperature are related by the equation of the state of an ideal gas:

$$p = \rho RT/M_a, \quad (5)$$

where R is the universal gas constant.

For small values of the current in the arc (see Table 1) and the absence of an external magnetic field, to describe the electrical part, it is enough to consider the equation for the electric field potential φ [17]:

$$-\nabla\cdot\left(\sigma(T)\nabla\varphi + \frac{\partial(\varepsilon_0\varepsilon_r\nabla\varphi)}{\partial t}\right) = 0, \quad (6)$$

where σ(T) is the temperature-dependent electric conductivity, ε_0 is the electrical constant, and ε is the relative permittivity. Relationship between potential and electric field strength $\mathbf{E} = -\nabla\varphi$, current density is defined as $\mathbf{j} = \sigma(T)\mathbf{E}$.

Boundary conditions and initial conditions. Depending on the simulation scenario (LF or HM), two types of setting the boundary conditions for equations (2)-(4) at the input boundary CD are considered. For both approaches, the inlet flow is not swirling and it is assumed that only the x component of the velocity $V_{x,in}$, perpendicular to the inlet section is nonzero.

For the LF approach, a velocity profile is set at the CD boundary corresponding to the steady flow between cylinders with the average velocity $V_{x,av}$ [28]. The gas temperature T_{in} is set too.

In the HM approach, disturbances from the downstream flow region can influence the solution at the subsonic inlet boundary [22,30,31]. Thus, the solution at the boundary is determined both by the given conditions and by the solution for the downstream flow field. In COMSOL Multiphysics, setting boundary conditions in this form correspond to the characteristics-based flow condition option. The specified boundary conditions include the values of the static pressure p_{in} and temperature T_{in}, as well as the Mach number at the boundary:

$$\mathrm{M}_{in} = V_{x,in}/\sqrt{\gamma R_g T_{in}}, \quad (7)$$

where γ is the specific heat ratio, R_g is the gas constant.

It should be noted that in order to match the flow rates of the plasma-forming gas for cases A and B through the inlet section (with accuracy of more than 98%), the velocity values differed for the LF and HM approaches. For the LF approach $V_{x,av} = 1\ \mathrm{m/s}$, for the HM approach $V_{x,in} = 1.075\frac{\mathrm{m}}{\mathrm{s}}$, $\mathrm{M}_{in} = 0.0031$.

The characteristic Reynolds numbers are given in Table 1. For cases A and B, Re is determined by the characteristic height of the inlet $H = R_c - R_e = 6\ mm$, and for case C by the channel radius R_c.

At the exit boundary, for all approaches, the static pressure $p_{out} = 1\,atm$ was considered known, and the change in temperature along the normal n to the surface was assumed to be zero

$$\left.\frac{\partial T}{\partial n}\right|_{out} = 0. \quad (8)$$

All solid surfaces (channel walls, electrode surfaces, channel end in the expansion area) were considered to be thermally insulated.

For calculation cases A and B (Table 1), a two-dimensional axisymmetric problem is considered. One of the electrodes is the end surface of the cylinder located in the channel. The end surface area of the cylinder is $S_E = 0.0314\,m^2$. The arc is "rigidly" attached to the electrode at the AB boundary. On this boundary, the condition is set

$$\int_S \mathbf{j} \cdot \mathbf{n_u}\, dS = I. \quad (9)$$

Here, $\mathbf{n_u}$ is the unit normal, and S is the surface area of the electrode. The second electrode is grounded. The current strength changes according to the law

$$I = I_0 \cdot \sqrt{2}\, sin(2\pi f_0 t), \quad (10)$$

where I_0 is the current RMS, $f_0 = 50\,Hz$.

For case C, the problem is three-dimensional. The electrode is a ring (see Fig. 1, AB boundary in scheme 2) on the inner surface of the channel. In this case, the only arc root is the "working" part, not the whole ring. The root area is $S_s = 0.0004\,m^2$. The current density is assumed to be constant over the root area and equal to $\boldsymbol{J}$. According to (9) $\boldsymbol{J} = I/S_s$. The current changes according to (10). The root moves according to the law discussed in the section below. One complete revolution takes approximately 100 ms.

Arc root motion in the 3D setting. In the absence of an external magnetic field, the typical value of the angular velocity of arc root rotation is ω~60 rad/s. A typical set of experimental data on the change in the arc root angle ϕ with time is shown in Fig. 2. For each time interval of 10 ms, the root rotates by about 36 degrees, making a complete revolution in about 100 ms. The law of angle change with time is repeated every 10 ms and is essentially non-linear (Fig. 2) due to an additional hopping movement of the attachment by about 0.2 rad (not shown in the figure).

The hybrid simulation algorithm includes a differential equation of motion of the arc root, describing the averaged experimental data. A differential equation of the arc root motion has been obtained using the modified algorithm of generative model design [25].

GMD involves the use of a multi-criteria evolutionary optimization algorithm to select the equation that most accurately reproduces the data. The algorithm contains single-criteria and multi-criteria steps.

The single-criteria step operates with a set of tokens representing possible "building blocks" of the future equation. Tokens are parameterized functions, for example, trigonometric, and differential operators of different orders.

The crossing and mutation and regularization operators are defined for a single-criteria algorithm. The crossing operator is the exchange of terms between equations-individuals. The mutation is represented by two operators – replacement of the whole term in the equation or one factor with a given probability. The cross-over operator is the terms exchanged between the equation-individuals. The regularization operator uses sparse regression to determine the shortest expression from a given set of terms with minimal discrepancy. At the same time, terms with a coefficient less than the specified one are removed from the equation. The single-criteria algorithm works for each of the equations on the Pareto front of the multi-criteria algorithm.

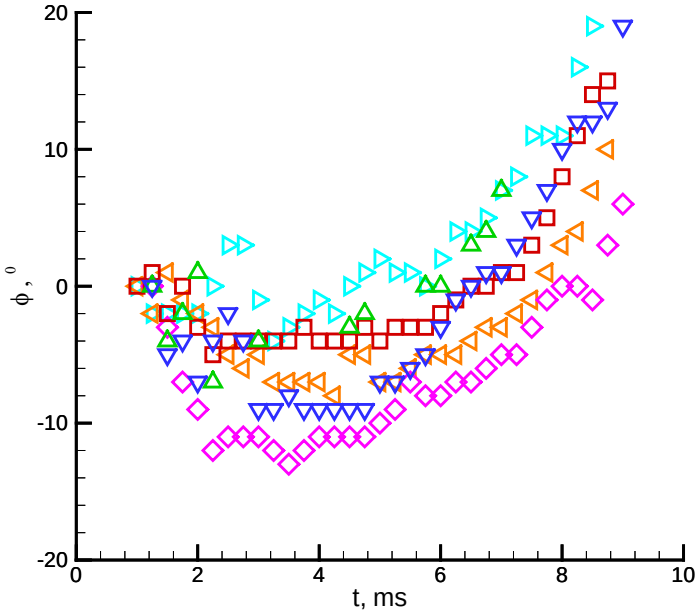

Fig. 2. An example of experimental data on the motion of an arc root. Different symbols and colors correspond to different measurements

A multi-criteria step is an update of a set of Pareto-nondominable solutions in the space of accuracy and complexity criteria. Accuracy in this case is the difference between a randomly selected term and all the others, that is, an analogue of the discrepancy. The second criterion is complexity, the number of non–zero terms in the equation. Thus, an equation with a minimum discrepancy is chosen for each number of terms from a given interval. After the construction of the Pareto fronts, a given number of nondominable levels is saved (the level, in this case, is the ordinal number of the equation sorted by discrepancy for a given number of terms) and a single-criterion step is performed for each equation, followed by the reconstruction of the front at the completion of all single-criterion steps.

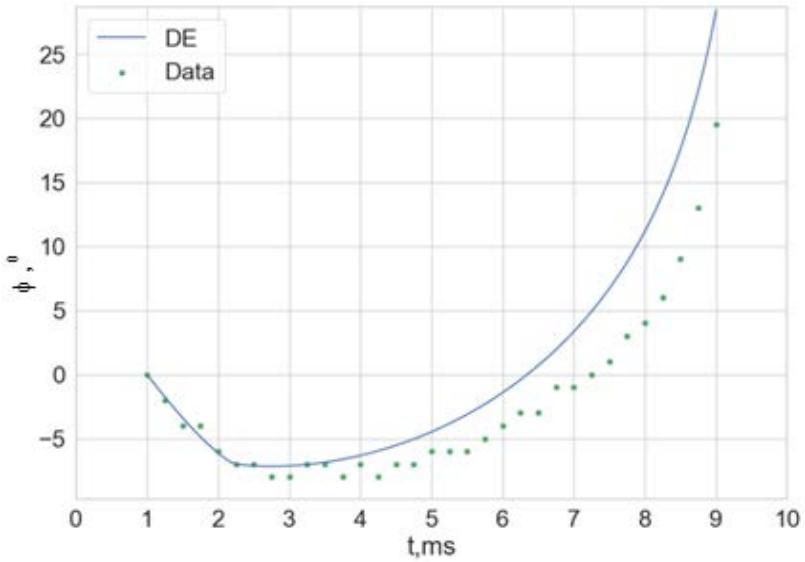

Fig. 3. Data (points) and solutions of the obtained differential equations (12)

For the equation of arc motion, the equation was sought in the form of a second-order equation

$$F(\phi'', \phi', \phi, t, f) = 0. \quad (11)$$

With due regard to the impact of external factors $f_1 = sin(2\pi f_0 t)$ or $f_2 = cos(2\pi f_0 t)$.

To restore the arc equation, median values of the angular deviation distribution at each moment of time were taken for the entire series of experiments. The median arc for restoring the equation is shown in Fig. 3.

The restored equation has the form

$$0.375181\phi' + 251.559\phi + 150.584\phi\, cos(2\pi f_0 t) + 47.4799 = sin(2\pi f_0 t)\phi' \quad (12)$$

The equation (12) solution was obtained using the scipy.odeint package is shown in Fig. 3.

Equation (12) is included in a hybrid model for calculating a plasma torch implemented in the COMSOL Multiphysics environment. In order to reduce the computational time, the solution of equation (12) is divided into two-time intervals, each of which is approximated by a polynomial of power 11.

Features of numerical implementation of the model in COMSOL Multiphysics environment. The COMSOL Multiphysics 6.0 package has been used to solve the hybrid problem of the flow in an AC plasma torch. The main computation parameters are summarized in Table 2.

Table 2 Computation parameters

Case	Time step, s	DOFs	Mesh elements	Damping factor	Tolerance	Computation time, h
A	2e-4	855265	195805	0.9	0.005	24
B	2e-4	855265	195805	Automatic	0.005	53
C	Automatic	95172	71794	1 (E) 0.8 (GH)	0.01	148

The finite element method is used to discretize differential equations by spatial coordinates in the COMSOL Multiphysics program. First order polynomials are used to calculate the weight and interpolation functions when processing both gas-dynamic variables (equations (2)-(4)) and electric potential (equation (6)). An implicit finite-difference scheme is used to discretize time derivatives. The calculations employ an IDA (Implicit Differential-Algebraic) solver based on the BDF (Backward differentiation formula) approach. The second-order time approximation is set in the settings. Time step selection option for case C is automatic. For cases A and B, the time step parameters and the mesh size were chosen on the basis of previous calculations [17] and an additional study of the influence of these parameters on the resulting solution. The damping factor in the Newton-Raphson method for solving the nonlinear problems is indicated in Table 2. A Fully Coupled approach is used for cases A and B, based on the Jacobian calculation for the general system of equations (2)-(4). In calculation C, the Segregated setting is used, which assumes the calculation of the Jacobian separately for the gas-dynamic together with the thermal (GH) part and electrical (E) part of the problem. The solution of algebraic equations is performed by the Pardiso solver. The calculations were carried out by the resources of the supercomputer cluster of the SCC "Polytechnic" on one computing node containing two Intel Xeon E5–2697 v3 CPUs.

An artificial conductivity of 235 S/m was used to initialize the arc discharge between the electrodes in cases A and B. By 10 milliseconds, its contribution to the total conductivity was zero. In case C, a volumetric energy source with a power of 500 W was set. Using the step function, this source was turned off 0.05 seconds after the start. The total time of the physical process was 1.5s.

4. Flow in a plasma torch with an end electrode

This section presents the results of simulations for cases A and B of the axisymmetric problem, which differ in the scenarios for modeling the flow of a compressible medium in the COMSOL Multiphysics package. Case A assumes using the Laminar Flow module with the Compressible Flow option. Case B involves using the High Mach Number Flow module. Figure 4 shows the maximum value of overpressure (over atmospheric pressure) in the flow area. It is seen that the maximum pressure deviation from the atmospheric pressure set at the boundary does not exceed 0.4%. At the same time, the maximum pressure values for case B are somewhat lower.

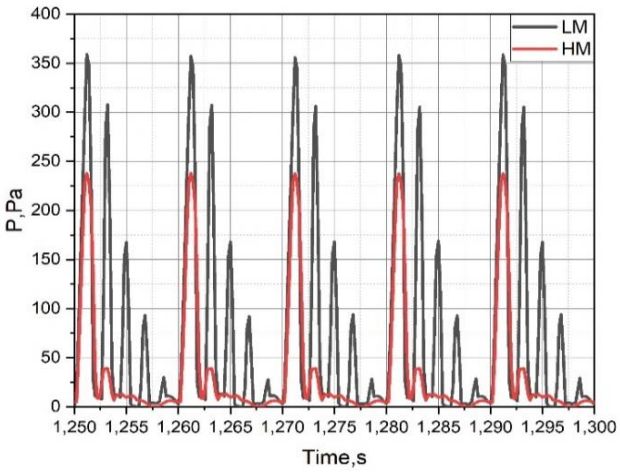

Fig. 4. The maximum value of overpressure in the flow area for simulation cases A (LM legend) and B (HM legend)

Figure 5 shows the axial distributions of temperature (Fig. 5a) and velocity (Fig. 5b) for cases A and B corresponding to the times when the value of the current in the arc is minimal *I=0* and maximal $I = \sqrt{2}I_0$. At the moment of the maximum current, the temperature in the channel rises to 6500K. In the region of the channel, the temperature weakly depends on the longitudinal coordinate. The discrepancy between calculation cases A and B in terms of the maximum temperature observed in the flow region does not exceed 2%. In the jet expansion region behind the plasma torch channel, the gas temperature and velocity oscillate in space [17,32]. The positions of the maxima and minima on the axial temperature distribution are close but do not coincide for cases A and B.

As discussed in Section 2, with an increase in temperature from 300 (inlet) to 6500 K for a simplified formulation of the problem, an increase in the flow velocity by a factor of 21.7 can be expected. The inlet velocity is near 1m/s (see Table 1). The maximum observed velocity is 20.7 m/s in case A and 17.5 m/s in case B. The maximum velocity is reached in the vicinity of the channel outlet. The velocity distributions in the cases under consideration are similar by quality. The most significant difference is manifested for the moment of minimum current in the region of the channel adjacent to the electrode. For case A, a stagnation point with zero velocity appears on the velocity profile. The velocity field shows an "instantaneous" circulation area at the given time behind the electrode. For other moments of time, the area of backward flow is lacking [32]. For case B, this area is not observed for any moments.

The fields of velocity and temperature for cases A and B and the moment of maximum current are shown in Figs. 6 and 7. It can be seen that the spatial variations of the parameters in both cases are close.

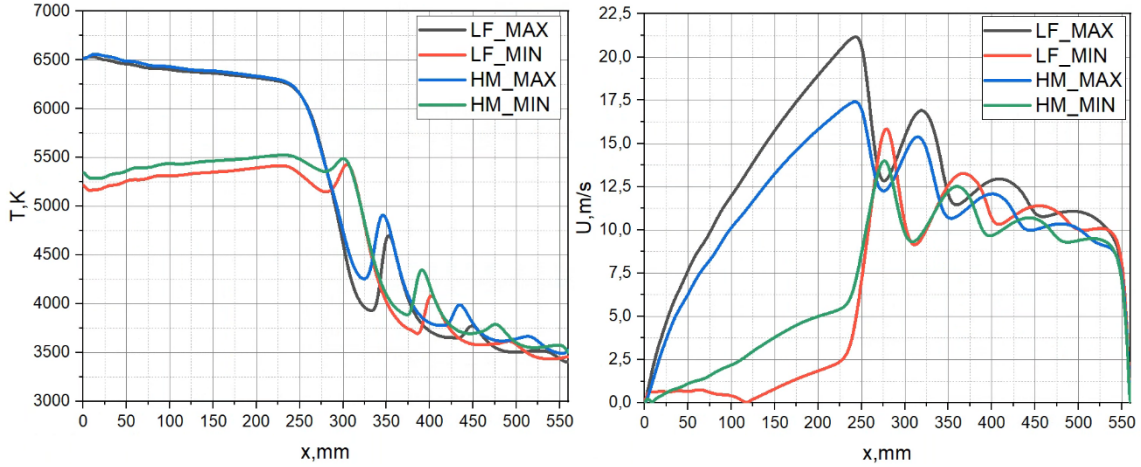

Fig. 5. Axial distributions of temperature (a) and velocity (b) for cases A (LF legend) and B (HM legend) corresponding to the moments of the minimal and maximal current value in the arc (MIN and MAX legends).

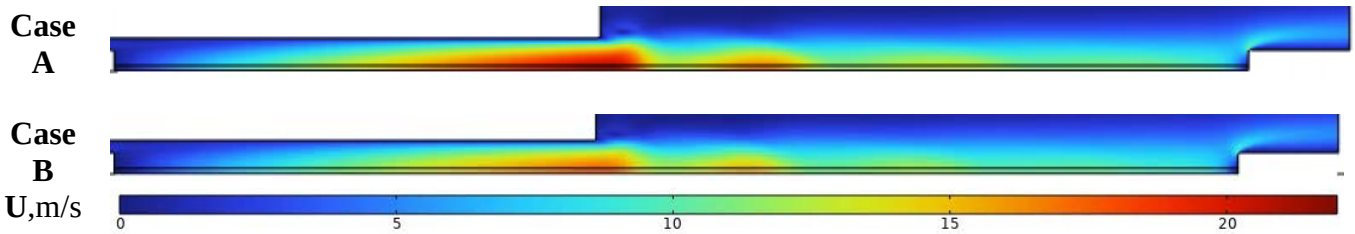

Fig. 6. Velocity fields for cases A and B and the moment of maximum current

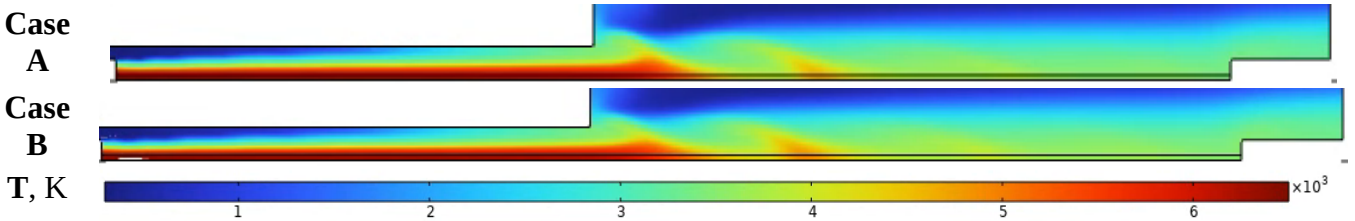

Fig. 7. Temperature fields for cases A and B and the moment of maximum current

The main difference between cases A and B is the behavior of the velocity at the inlet boundary. For case A (LF approach), the velocity value does not fluctuate, while in case B (HM approach), the fluctuations are significant. The latter is related to the specific character of the HM approach [22] and boundary conditions settings (see section 3). The internal tests show that the presence of such fluctuations is independent of the mesh size. For the problem under consideration with a nonstationary energy supply resulting in a significant change in temperature in space and time, such oscillations of parameters in a subsonic flow can be physical but require experimental verification.

Thus, to estimate the flow parameters both in the channel (except the region adjacent to the inlet boundary) and in the jet expansion region, any of the discussed approaches (LF or HM) can be used. However, the experience of solving similar problems in the COMSOL Multiphysics environment with different data (different values of velocity and gas flow rate at the inlet boundary) suggests that the simulation using the HM approach is more stable from a computational point of view.

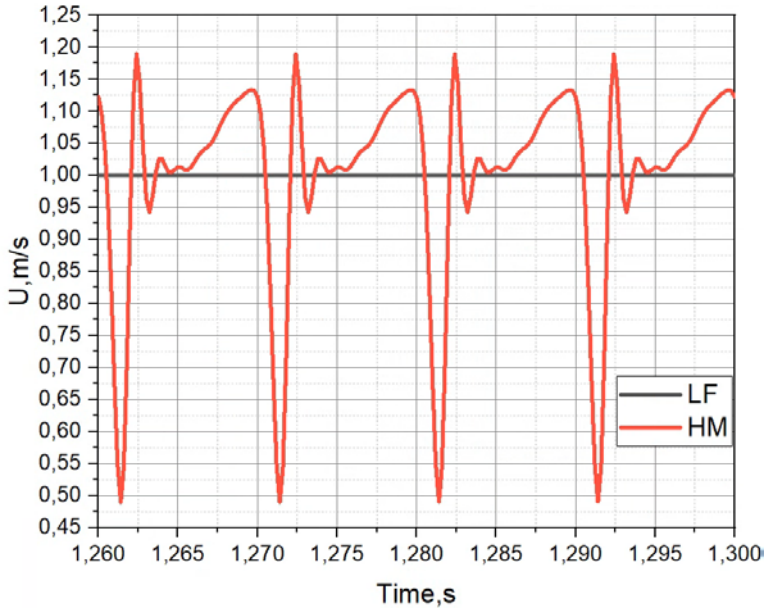

Fig. 8. Average velocity over the section at the inlet boundary for cases A (LM legend) and B (HM legend)

5. The flow in the plasma torch with regard to the arc root movement

In the previous section, the flow in the plasma torch, one of the electrodes of which is the end face of an inner cylinder with a radius of 10 mm (see Fig. 1), had been considered. The arc root is "rigidly" attached to the electrode surface (case B, Table 1). This formulation of the problem predetermines the symmetry of the variation in parameters relative to the axis. The statement of the problem in case C (Table 1) is more complex, assuming that (i) the electrode surface coincides with the surface of the cylindrical channel with a radius of 16 mm (see Fig. 1) and (ii) the arc root moves along this surface according to equation (12). Taking into account the displacement of the arc root effects a significant change in the gas-dynamic flow pattern.

Figure 9 shows the temperature distribution for different time moments in section X=0, which coincides with the electrode for case B and with the end of the hollow electrode for case C. As noted above, for case B, the picture is symmetrical about the axis with a maximum temperature of about 6500K. For case C, the location of the temperature maximum coincides with the location of the center of the arc root. The maximum temperature in the vicinity of the root center exceeds 8000 K. The temperature difference for cases B and C is explained mainly by the difference in current density and partially by the difference in flow rate (see Table 1). The flow rate affects the arc voltage drop [32]. The current density for case C turns out to be higher due to the smaller root area (Fig. 10), respectively, and the Joule heating of the arc near such a root is also higher. In the remaining sections of the channel downstream, the temperature distributions for case C retain their asymmetric form (Fig. 11). In sections X=120mm (middle of the channel) and X=240mm (outlet from the channel), the maximum observed temperature values are close to case B. In the outlet section of the channel, the temperature value averaged over the entire section is close to case B (Table 3) and is about 3900K.

Table 3. Average values of parameters in the section X=240 (outlet of the channel)

	Velocity, m/s	Temperature, K
Case B	10.283	3982.7
Case C	16.879	3874.7

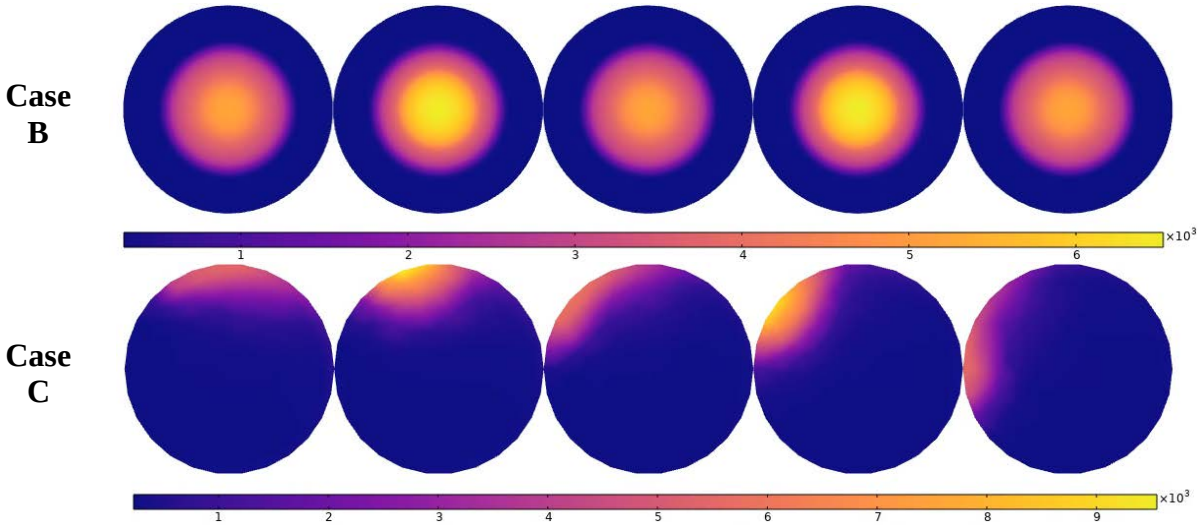

Fig. 9. Distribution of gas temperature (K) in section X=0 for different moments of time (t=0, $t=T_0/4$, $t=T_0/2$, $t=3T_0/4$, $t=T_0$. T_0 = 0,02 s.). Case B on the top, case C on the bottom

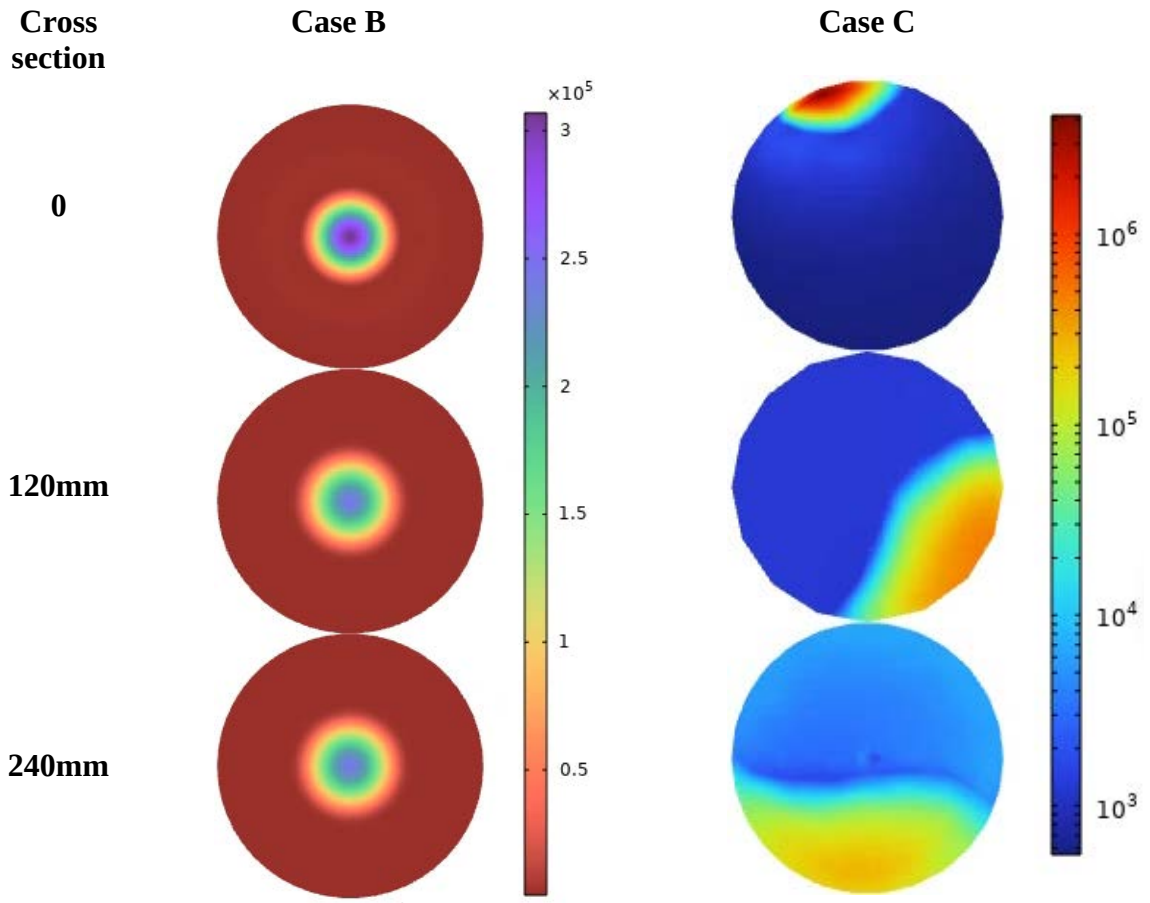

Fig. 10. Current density (A/m^2) at the moment of the maximum current in the sections X=0, X=120mm, X=240mm (exit from the channel). Case B is on the left, case C on the right.

The distributions of the remaining parameters for the calculation case C are also asymmetric (e.g. Fig. 10). The gas velocity in section X=0 in the vicinity of the arc attachment spot exceeds 15 m/s, in most of the sections the velocity is less than 5 m/s. The maximum velocity averaged over the cross-section is reached at the outlet of the channel (Table 3). For case B the velocity distributions in the sections are symmetrical, and the

maximum velocity in the outlet section is lower compared to case C. This difference is due to the difference in flow rates for cases B and C (see Table 1).

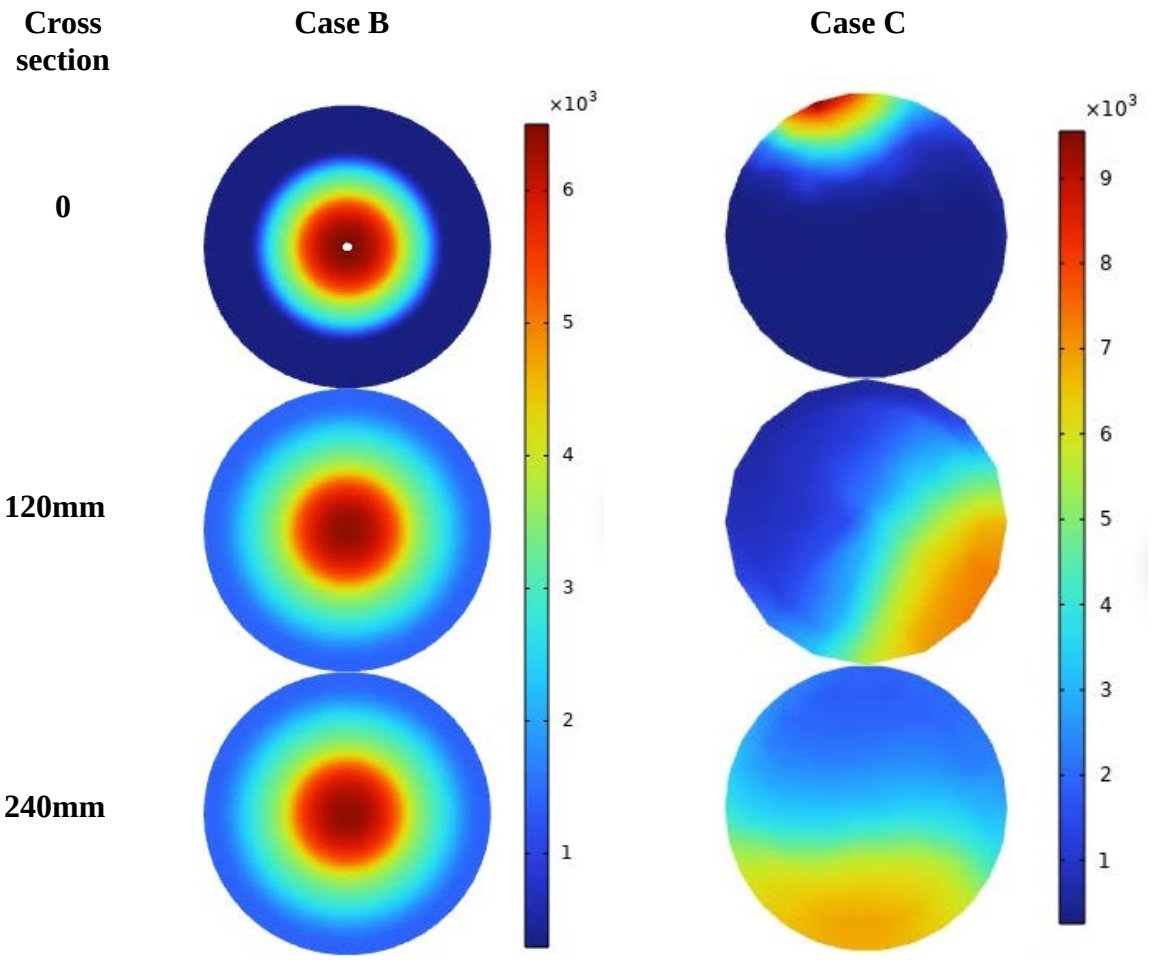

Fig. 11. Gas temperature (K) at the moment of the maximum current in the sections X=0, X=120mm, X=240mm (exit from the channel). Case B is on the left, case C on the right

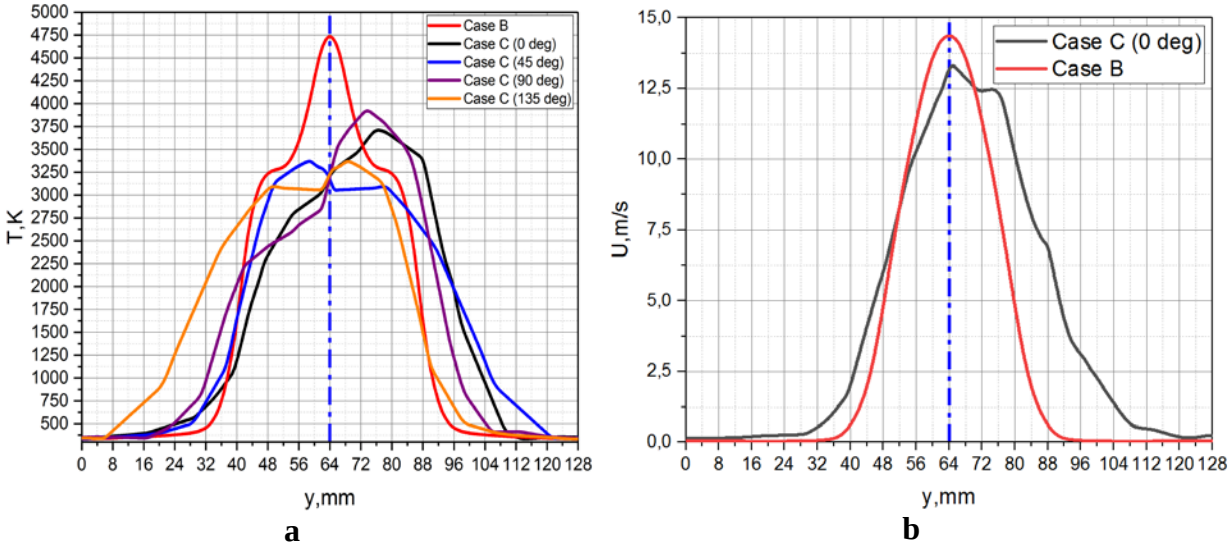

Fig. 12. Radial distribution of temperature (a) and velocity (b) in section X=300 mm

From the point of view of plasma chemistry and technologies for the synthesis of nanostructured materials, the parameters of the heated gas, including the jet dimensions in the expansion region outside the channel are of great importance. For case B, the temperature in the jet on the axis does not fall below 3500K, the characteristic transverse size of the jet Y_{ch} in section X=300mm (Fig. 12a), corresponding to the temperature drop to 1000K, is about $1.6R_c$. Rotation of the arc root leads to broader distribution of temperature with a lower maximum. The characteristic transverse size of the jet is about $Y_{ch}=2R_c$. The radial distribution of velocity is also broader (Fig. 12b).

6. Conclusions

Thermal plasma generators are in demand for many modern technologies for the synthesis of nanostructured and powder materials, as well as materials with special performance properties. Alternating current electric arc plasma torches are promising sources of thermal plasma.

The development of electric arc plasma torches for each specific technology requires an assessment of the plasma parameters. The description of the processes of heating the plasma-forming gas by alternating electric current, its ionization, gas-dynamic acceleration in the plasma torch channel, and the outflow of a high-enthalpy jet into the background gas is a non-trivial problem that can only be solved by numerical methods. Taking into account the complexity of the problem, the development of the corresponding computational model is carried out in stages.

In this paper, we continue the development of a hybrid model of an AC plasma torch in the COMSOL Multiphysics environment proposed in [17]. The model involves calculating the parameters of the electric field, determining the heating power of the plasma-forming medium, and solving the system of Navier-Stokes equations to determine the density, velocity, and temperature of the gas. The electrical and gas-dynamic subproblems are related through the temperature-dependent conductivity of the medium, which affects the local current density and Joule heating. Air is considered a plasma-forming medium, the thermophysical parameters of which, including the molar mass, depending on temperature.

In the presented study, special attention is paid to the correct consideration of the compressibility factor of the plasma-forming gas. The compressibility of a medium can be taken into account within the COMSOL Multiphysics package using the Laminar/Turbulent Flow module with the Compressible Flow option, or the High Mach Number Flow module. For the first time, the results of applying these modules to solve the problem of essentially subsonic flow of a compressible gas with energy release into the flow are compared. It is shown that the results obtained using different computational scenarios are close to each other. The temperature distributions in the flow region practically coincide. The gas velocity distributions are close, however, the maximum value of the flow velocity achieved at the moment of maximum current differs by 17%. Thus, both approaches (modules) can be used to estimate the flow parameters. However, the use of the High Mach Number Flow module showed greater computational stability of the computational algorithm implemented in it when the set of initial data changes.

As an element of the hybrid model, the present paper takes into account the process of arc root motion along the electrode surface. For the first time, to describe this process, it is proposed to use the differential equation of motion of the arc root, reconstructed from the available experimental data using the generative model design method. Taking into account the root motion required the solution of a three-dimensional problem. The results of calculating the spatial parameter distributions differ significantly from the symmetric distributions observed when the motion of the arc root is not taken into account. Asymmetry in the parameter distributions is observed both along the entire length of the channel and in

the region of jet expansion. Accounting for the arc root motion is an important element of the plasma torch model, bringing the simulation results closer to the flow pattern observed in reality.

References

1. Mostaghimi J, Boulos MI. Thermal Plasma Sources: How Well are They Adopted to Process Needs? *Plasma Chem Plasma Process.* 2015;35: 421-436.
2. Fulcheri L, Fabry F, Takali S, Rohani V. Three-phase AC arc plasma systems: a review. *Plasma Chem Plasma Proc*. 2015;35: 565-85.
3. Klimenko GK, Kuzenov VV, Lyapin AA, Ryzhkov SV. *Calculation, modeling and design of low-temperature plasma generators.* Publishing House of MSTU; 2021. (In Russian)
4. Gautier M, Rohani V, Fulcheri L, Direct decarbonization of methane by thermal plasma for the production of hydrogen and high value-added carbon black. *International Journal of Hydrogen Energy*. 2017;42(47): 28140-28156.
5. Jensen R, van der Eijk C, Wærnes AN. Production of Sustainable Hydrogen and Carbon for the Metallurgical Industry. *Mater. Proc*. 2021;5(1): 67.
6. Juan L, Fangfang H, Yiwen L, Yongxiang Y, Xiaoyan D, Xu L. A New Grade Carbon Black Produced by Thermal Plasma Process. *Plasma Science & Technology*. 2003;5(3): 1815-1819.
7. Xie Z, Tang Z, Zhang D, Kang N, Su X, Yang B, Dai Y, Liang F. Hydrogen arc plasma promotes the purification and nanoparticle preparation of tungsten. *Int. J. Refract. Met. Hard Mater.* 2022;105: 105815.
8. Shekhovtsov VV, Skripnikova NK, Volokitin OG. Phase transitions in SiO2 nanopowder synthesized by electric arc plasma. *IEEE transactions on plasma science*. 2021;49(9): 2618-2623.
9. Rat V, Chazelas C, Goutier S, Keromnes A, Mariaux G, Vardelle A. In-flight mechanisms in suspension plasma spraying: issues and perspectives. *J. Therm. Spray Tech.* 2022;31: 699-715.
10. Wang H, Zeng M, Liu J et al. One-step synthesis of ultrafine WC-10Co hardmetals with VC/V2O5 addition by plasma assistedmilling, *Int. J. Refract.Met. HardMater*. 2015;48: 97-101.
11. Wei CB, Song XY, Fu J et al. Microstructure and properties of ultrafine cemented carbides-differences in spark plasma sintering and sinter-HIP. *Mater. Sci. Eng. A.* 2012;552: 427-433.
12. Sivaprahasam D, Chandrasekar SB, Sundaresan R. Microstructure and mechanical properties of nanocrystalline WC-Co consolidated by spark plasma sintering. *Int. J. Refract. Met. Hard Mater.* 2007;25(2): 144-152.
13. Qi J, Luo Y, Yin Y, Dai X. Preparation of Ultra-fine Aluminum Nitride in Thermal Plasma. *Plasma Science & Technology.* 2002;4(4): 1417.
14. Surov AV, Popov SD, Popov VE, Subbotin DI, Serba EO, Spodobin VA, Nakonechny GhV, Pavlov AV. Multi-gas AC plasma torches for gasification of organic substances. *Fuel.* 2017;203: 1007-1014.
15. Rutberg PhG, Nakonechny GhV, Pavlov AV, Popov SD, Serba EO, Surov AV. AC plasma torch with a H2O/CO2/CH4 mix as the working gas for methane reforming. *J. Phys. D: Appl. Phys.* 2015;48(24): 245204.
16. Baeva M, Benilov MS, Almeida NS, Uhrlandt D. Novel nonequilibrium modelling of a DC electric arc in argon. *J. Phys. D: Appl. Phys.* 2016;49(24): 245205.
17. Bykov NY, Obraztsov NV, Kobelev AA, Surov AV. Modeling of an AC Plasma Torch - Part I: Electrical Parameters and Flow Temperature. *IEEE Transactions on Plasma Science.* 2021;49(3): 1017-1022.

18. Ivanov DV, Zverev SG. Mathematical Simulation of Plasma Processes in a Radio Frequency Inductively Coupled Plasma Torch in ANSYS Fluent and COMSOL Multiphysics Software Packages. *IEEE Transactions on Plasma Science.* 2022;50(6): 1700-1709.
19. Ivanov DV, Zverev SG. Mathematical Simulation of Processes in Air ICP/RF Plasma Torch for High-Power Applications. *IEEE Transactions on Plasma Science*. 2020;48(2): 338-342.
20. Rehmet C, Fabry F, Rohani V, Cauneau F, Fulcheri L. A comparison between MHD modeling and experimental results in a 3-phase AC arc plasma torch: influence of the electrode tip geometry. *Plasma Chem. Plasma Process*. 2014;34: 975-996.
21. Zhou X, Chen X, Ye T, Zhu M. Large eddy simulation on the flow characteristics of an argon thermal plasma jet. *Plasma Sci. Technol*. 2021;23(12): 125405.
22. *COMSOL AB, COMSOL Multiphysics-CFD Module, User's Guide*. 2022.
23. Sambou F, Gonzalez JJ, Benmouffok M, Freton P. Theoretical study of the arc motion in the hollow cathode of a dc thermal plasma torch. *J. Phys. D: Appl. Phys*. 2022;55(2): 025201.
24. Benilov MS. Understanding and modeling plasma–electrode interaction in high pressure arc discharges: a review. *Phys. D: Appl. Phys*. 2008;41(14): 144001.
25. Maslyaev M, Hvatov A, Kalyuzhnaya AV. Partial differential equations discovery with EPDE framework: Application for real and synthetic data. *Journal of Computer Science.* 2021;53: 101345.
26. Bykov NY, Hvatov AA, Kalyuzhnaya AV, Boukhanovsky AV. A method for reconstructing models of heat and mass transfer from the spatio-temporal distribution of parameters. *Technical Physics Letters*. 2021;47: 9-12. (In Russian)
27. Bykov N, Hvatov A, Kalyuzhnaya A, Boukhanovsky A. A method of generative model design based on irregular data in application to heat transfer problems. *Journal of Physics: Conference Series.* 2021;1959: 012012.
28. Loitsyansky LG. *Mechanics Fluid Gas*. Moscow: Nauka; 1973. (In Russian)
29. *Calculation of near- and supersonic technologies in COMSOL Multiphysics*. Available from: https://www.COMSOL.ru/video/sub-and-supersonic-flows-in-COMSOL-webinar-ru. [Accessed 18th July 2022] (in Russian).
30. Poinsot T, Veynante D. *Theoretical and Numerical Combustion.* Edwards; 2005.
31. Larsson J. *Numerical Simulation of Turbulent Flows for Turbine Blade Heat Transfer Applications*. *Ph.D. thesis.* Chalmers University of Technology; 1998.
32. Bykov NY, Obraztsov NV, Kobelev AA, Surov AV. Modeling of an AC Plasma Torch – Part II: Gasdynamic Pattern and Effect of Flow Rate. *IEEE transactions on plasma science.* 2021;49(3): 1023-1027.

THE AUTHORS

Obraztsov N.V.
e-mail: nikita.obrazcov@mail.ru
ORCID: 0000-0003-1107-3259

Bykov N.Y.
e-mail: nbykov2006@yandex.ru
ORCID: 0000-0003-0041-9971

Hvatov H.A.
e-mail: alex_hvatov@itmo.ru
ORCID: 0000-0002-5222-583X

Maslyaev M.M.
e-mail: mikemaslyaev@itmo.ru
ORCID: 0000-0001-5595-0802

Surov A.V.
e-mail: alex_surov@mail.ru
ORCID: 0000-0003-4671-5741